Published in final edited form as:
*Toxicol Appl Pharmacol*. 2014 September 1; 279(2): 220–229. doi:10.1016/j.taap.2014.06.010.

# Comparative toxicity and efficacy of engineered anthrax lethal toxin variants with broad anti-tumor activities

**Diane E. Peters**[a,b], **Benjamin Hoover**[c], **Loretta Grey Cloud**[a], **Shihui Liu**[c], **Alfredo A. Molinolo**[d], **Stephen H. Leppla**[c], and **Thomas H. Bugge**[a]

[a]Proteases and Tissue Remodeling Section, Oral and Pharyngeal Cancer Branch, National Institute of Dental and Craniofacial Research, National Institutes of Health, Bethesda, MD, USA

[b]Program of Pharmacology and Experimental Therapeutics, Tufts University School of Medicine, Boston, MA, USA

[c]Laboratory of Parasitic Diseases, National Institute of Allergy and Infectious Diseases, National Institutes of Health, Bethesda, Maryland, USA

[d]Oral and Pharyngeal Cancer Branch, National Institute of Dental and Craniofacial Research, National Institutes of Health, Bethesda, MD, USA

## Abstract

We have previously designed and characterized versions of anthrax lethal toxin that are selectively cytotoxic in the tumor microenvironment and which display broad and potent anti-tumor activities *in vivo*. Here, we have performed the first direct comparison of the safety and efficacy of three engineered anthrax lethal toxin variants requiring activation by either matrix-metalloproteinases (MMPs), urokinase plasminogen activator (uPA) or co-localized MMP/uPA activities. C57BL/6J mice were challenged with six doses of engineered toxins via intraperitoneal (I.P.) or intravenous (I.V.) dose routes to determine the maximum tolerated dose for six administrations (MTD6) and dose-limiting toxicities. Efficacy was evaluated using the B16-BL6 syngraft model of melanoma; Mice bearing established tumors were treated with six I.P. doses of toxin and tumor measurements and immunohistochemistry, paired with terminal blood work, were used to elaborate upon the anti-tumor mechanism and relative efficacy of each variant. We found that MMP-, uPA- and dual MMP/uPA- activated anthrax lethal toxins exhibited the same dose-limiting toxicity; dose-dependent GI toxicity. In terms of efficacy, all three toxins significantly reduced primary B16-BL6 tumor burden, ranging from 32%–87% reduction, and they also delayed disease progression as evidenced by dose-dependent normalization of blood work values. While target organ toxicity and effective doses were similar amongst the variants, the dual MMP/uPA-activated anthrax lethal toxin exhibited the highest I.P. MTD6 and was 1.5–3-fold better tolerated than the single MMP- and uPA-activated toxins. Overall, we demonstrate that this dual MMP/uPA-activated anthrax

Address correspondence and reprint requests to: Thomas H. Bugge, Ph.D., Proteases and Tissue Remodeling Section, Oral and Pharyngeal Cancer Branch, National Institute of Dental and Craniofacial Research, National Institutes of Health, 30 Convent Drive, Room 211, Bethesda, MD 20892, Phone: (301) 435-1840, Fax: (301) 402-0823, thomas.bugge@nih.gov.

lethal toxin can be administered safely and is highly effective in a preclinical model of melanoma. This modified bacterial cytotoxin is thus a promising candidate for further clinical development and evaluation for use in treating human cancers.

### Keywords

prodrug; cancer; melanoma; bacterial cytotoxin; protease

## Introduction

Development of anti-cancer agents that are specifically activated in the tumor microenvironment is an appealing strategy due to the potential for reduced off-target toxicity. One means to achieve tumor-specific activation is to exploit the fact that many tumors overexpress proteases that are present at low levels in normal tissues (reviewed in (Andreasen et al., 1997; Bugge, 2003; Duffy et al., 2011; Kontos and Scorilas, 2012; Roy et al., 2009)). Two classic examples of tumor-over-expressed proteases are matrix metalloproteinases (MMPs) and urokinase plasminogen activator (uPA) and we have previously generated and characterized versions of anthrax toxin requiring proteolytic activation by either, or both, of these enzymes (Liu et al., 2000; Liu et al., 2001; Liu et al., 2005).

Anthrax lethal toxin is a binary toxin secreted by *Bacillus anthracis*. It is comprised of two individual proteins: a toxin receptor-binding moiety, anthrax protective antigen (PrAg), and a cytotoxin, anthrax lethal factor (LF) (Liu et al., 2003a). Individually PrAg and LF are non-toxic entities and in order for cellular internalization and subsequent cytotoxicity to occur, PrAg must first bind to one of two ubiquitous cell surface receptors, tumor endothelial marker 8 (TEM8, also ANTXR1) or capillary morphogenesis gene 2 (CMG2, also ANTXR2) (Bradley et al., 2001; Liu et al., 2009; Scobie et al., 2003). Once receptor-bound, PrAg is cleaved and activated by furin or furin-like pro-protein convertases at the sequence $^{164}$RKKR$^{167}$ generating an activated PrAg monomer that remains receptor bound (Klimpel et al., 1992). Multiple PrAg monomers aggregate forming complexes capable of binding to LF and translocating it into the cytosol (Cunningham et al., 2002; Mogridge et al., 2002). LF is a zinc metalloproteinase that once internalized cleaves and inactivates mitogen-activated protein kinase kinases (MEKs), disrupting the extracellular signal-related kinase (ERK)/mitogen activated protein kinase (MAPK) pathway, ultimately resulting in cell death (Duesbery et al., 1998; Vitale et al., 1998; Vitale et al., 2000).

By altering the cleavage sequence required for proteolytic activation of PrAg, cytotoxicity can be redirected as internalization of LF, or related cytotoxins, will occur only in the presence of a specified proteolytic activity. Employing this principle, we have previously generated versions of PrAg requiring activation by MMPs (PrAg-L1) (Liu et al., 2000), uPA (PrAg-U2) (Liu et al., 2001), or co-localized MMP/uPA activities (IC-PrAg, consisting of two separate proteins, PrAg-L1-I210A and PrAg-U2-R200A) (Liu et al., 2005). Multiple studies have been performed, as summarized in Table 1, demonstrating that when these engineered PrAgs are co-administered with various cytotoxins, that significant anti-tumor

activity towards established tumors can be achieved in a variety of syngraft, xenograft and orthotopic models, highlighting the potential broad-spectrum therapeutic utility of these agents (Alfano et al., 2010; Liu et al., 2003b; Liu et al., 2005; Liu et al., 2008; Rono et al., 2006; Schafer et al., 2011; Su et al., 2007; Wein et al., 2013). These toxin combinations exert there anti-tumor effects through a variety of means including both direct tumor cell killing and killing of cellular components of the tumor stroma, including tumor vasculature (Alfano et al., 2008; Alfano et al., 2010; Liu et al., 2003b; Liu et al., 2008; Schafer et al., 2011).

While these highly similar toxin combinations all exhibit potent anti-tumor efficacies, simultaneously toxicities of varying severity have been reported with their use. A particularly striking toxicity was evident with systemic administration of PrAg-U2 + FP59 where in order to administer effective doses, without significant mortality, co-administration of the anti-inflammatory glucocorticoid, dexamethasone, was required (Rono et al., 2006; Su et al., 2007) (FP59 is a potent protein synthesis inhibitor composed of the N-terminal PrAg-binding domain of LF coupled to the enzymatic domain of *Pseudomonas aeruginosa* exotoxin A).

The present study was initiated to provide a detailed preclinical evaluation of the dose-limiting toxicities, comparative efficacy, and anti-tumor mechanisms associated with multiple systemic doses of PrAg-L1, PrAg-U2 and IC-PrAg, when co-administered with LF. Herein we identify that IC-PrAg + LF is, in fact, the best tolerated version. We describe in detail the dose-limiting toxicity associated with IC-PrAg + LF administration, dose-dependent GI toxicity, and further show that effective doses of this toxin towards established tumors can be administered far below where this dose-limiting toxicity is first encountered. This study demonstrates that IC-PrAg + LF is well-tolerated, highly effective, and is a promising candidate for further development as an anti-cancer agent.

## Materials and Methods

### Protein Purification

Recombinant anthrax protective antigens (PrAg) including: PrAg-WT (wild-type, furin-activated), PrAg-U2 (uPA-activated), PrAg-L1 (MMP-activated), IC-PrAg (dual MMP/uPA-activated, consisting of two individual proteins: PrAg-L1-I210A and PrAg-U2-R200A), PrAg-U7 (protease resistant), and recombinant anthrax lethal factors including: LF (wild-type) and LF-E687A (enzymatically-inactive, similar to previously used LF-E687C (Klimpel et al., 1994)) were generated and purified as previously described (Liu et al., 2000; Liu et al., 2001; Liu et al., 2003b; Liu et al., 2005; Park and Leppla, 2000). The LF used herein has the native N-terminal sequence: AGG.

### Animals

Female, 6–8 week old, C57BL/6J mice (The Jackson Laboratory, Bar Harbor, ME), weighing between 16–18 g, were used for all experiments. Animals were housed in an AAALAC-certified pathogen-free environment and all studies were performed in

accordance with protocols approved by the NIDCR Animal Care and Use Committee (Animal Study Proposal Numbers: 10-585 and 13-712).

### Comparative Evaluation of Toxicity

Mice received 6 injections of PBS or engineered anthrax lethal toxins via intraperitoneal (I.P.) or intravenous (I.V.) dose routes over the course of two weeks on a MWFx2 schedule. On study day 14, all surviving mice were euthanized, complete gross necropsies were performed and organs were collected and fixed for histopathological examination. All organs where toxicity has been previously reported for similar toxin combinations were included in our analysis [gastrointestinal (GI) tract (18, 19), spleen (18), adrenal gland (18), kidney (20), lung (20), liver (20), heart (20) and femur (7, 18)]. In addition, skin, mammary gland, salivary gland, thyroid gland, abdominal wall, quadriceps femoris muscle, pancreas, gall bladder, bladder, ovaries, uterus, sternum and spinal cord were analyzed. In this study, MTD6 was defined as the highest toxin concentration administered where no lethality was observed in a treated cohort of a minimum size of 10 mice. Comparison of survival data was performed using the Log-Rank test, two-tailed.

GI motility was assessed using an activated charcoal gavage assay. Specifically, mice were treated with 3 I.P. or I.V. doses of MMP-activated PrAg-L1 + LF on a MWF schedule, at either its MTD6, or at a dose 2-fold above its MTD6. Following the 3$^{rd}$ dose, mice were fasted for 20 hours and were then challenged with oral gavage of 150 μL of a 10% charcoal, 5% gum arabic slurry. Mice were euthanized 45 minutes (I.V.) or 60 minutes (I.P.) post-challenge, the GI tracts were harvested, charcoal transit through the small intestine was measured, and a GI motility factor was determined by dividing the length of charcoal transit (cm) by the length of the small intestine (cm).

### Comparative Evaluation of Efficacy

B16-BL6 melanoma cells were a kind gift from Dr. Isaiah J. Fidler (MD Anderson Cancer Center, Houston, TX), and were authenticated by continual assessment of cellular morphology at both low and high magnifications.

B16-BL6 cells ($5\times10^5$ per mouse) were injected in the mid-scapular subcutis. When tumors were established, actively growing and had reached a volume of 50–100 mm$^3$, the mice were divided into cohorts with equivalent mean tumor sizes. Each group contained a minimum of 10 mice. Mice received a total of 6 I.P. injections of either 400 μl PBS, or of engineered anthrax lethal toxin in 400 μl PBS. Eleven different engineered anthrax lethal toxin treatments were tested as listed in Figure 2G.

At the time of dosing, a blinded investigator weighed the mice and measured the longest and shortest tumor diameters with digital calipers (FV Fowler Company, Inc., Newton, MA). Tumor volume was estimated using the equation $\mathrm{V}=(\mathrm{length\,in\,mm}*(\mathrm{width\,in\,mm})^2)/2$ (Tomayko and Reynolds, 1989). Statistical significances of differences in tumor sizes were determined using the two-tailed Student's t-test.

Terminal blood collection was performed on all surviving mice on study day 14. Blood was collected via cardiac puncture, and was processed and submitted to the NIH Clinical Center

Department of Laboratory Medicine (Bethesda, MD) for complete blood count and a limited blood chemistry panel. A sham-treated, tumor-free, cohort of ten mice was analyzed in parallel to obtain disease-free blood work values.

### Comparative Evaluation of Anti-Tumor Mechanism

Tumors were harvested, fixed in 4% paraformaldehyde for 24 h, embedded in paraffin and sectioned. All slide images were captured using an Aperio T3 Scanscope and quantification was performed by a blinded investigator using Aperio Imagescope Software (Aperio Technologies, Vista, CA).

Percent necrosis was determined from hematoxylin and eosin (H&E) stained sections. Unstained sections were stained with a monoclonal rabbit anti-mouse PECAM-1 (Santa Cruz Biotechnology, Inc., Santa Cruz, CA) and a polyclonal rabbit anti-human Ki67 (Novocastra Laboratories, Ltd., Newcastle, UK), to quantify, respectively, differences in blood vessel density and alterations in cellular proliferation. TUNEL staining was performed using a TdT In Situ Apoptosis Detection Kit – TACS Blue Label (Trevigen Inc., Gaithersburg, MD) per manufacturer's instructions. Statistical significances of differences were calculated using the Student's t-test, two-tailed.

## Results

### Comparative Toxicity: Determination of MTD6

We first determined the maximum tolerated dose for six intraperitoneal (I.P.) administrations of the MMP-, uPA- and dual MMP/uPA-activated anthrax lethal toxins (Summarized in Table 2). As expected, we found that each of the engineered PrAgs was non-toxic when administered I.P. without cytotoxin (100 μg PrAg-XX) or when they were co-administered with an enzymatically-inactive cytotoxin, LF-E687A (100 μg PrAg-XX + 33 μg LF-E687A). We verified that proteolytic cleavage of the engineered PrAgs was required for subsequent LF-mediated toxicity *in vivo*, as an uncleavable, protease-resistant, variant of PrAg (PrAg-U7) (Liu et al., 2003b) was found to be non-toxic when administered at high doses with LF (100 μg PrAg-U7 + 33 μg LF) (Table 2).

The dual MMP/uPA-activated anthrax lethal toxin, IC-PrAg + LF, was identified as the best tolerated version, exhibiting the highest I.P. MTD6 (45 μg IC-PrAg + 15 μg LF). This was 3-fold improved from the I.P. MTD6 of the MMP-activated version (I.P. MTD6: 15 μg PrAg-L1 + 5 μg LF) and 1.5-fold improved from the uPA-activated version (I.P. MTD6: 30 μg PrAg-U2 + 10 μg LF). All three engineered anthrax lethal toxins were far better tolerated then wild-type anthrax lethal toxin, which resulted in 100% lethality following only 3 I.P. doses at a concentration of 15 μg PrAg-WT + 5 μg LF (Table 2).

While I.P. administration is routinely utilized for systemic dosing in mice, intravenous (I.V.) administration is a far more common route used for larger mammalian species, therefore, we next determined I.V. MTD6s for each of the engineered toxins (Table 3). Similar to I.P. administration, we found that when administered I.V., PrAg-L1 + LF was the least tolerated version (I.V. MTD6: 6 μg PrAg-L1 + 2 μg LF), while both PrAg-U2 + LF and IC-PrAg + LF exhibited a 2-fold increase in tolerance (I.V. MTD6s: 12 μg PrAg-U2 + 4 μg LF and 12

μg IC-PrAg + 4 μg LF). Again, all engineered toxins were far better tolerated than wild-type anthrax lethal toxin, which yielded 100% lethality when administered at a dose of 6 μg PrAg-WT + 2 μg LF (Table 3).

Unexpectedly, mortality was observed when high I.V. doses of the engineered PrAgs were administered without LF. Specifically, six I.V. doses of 50 μg PrAg-L1, PrAg-U2 or IC-PrAg alone, resulted in 40%, 25% and 20% lethality respectively (Table 3). While unanticipated, this phenomenon of PrAg-alone toxicity is unlikely to be therapeutically relevant as the doses where PrAg alone toxicity occurred far exceed the MTD6s identified for I.V. administration of PrAg in conjunction with LF; however, determining the threshold at which the engineered PrAg can be safely administered alone may be an appropriate first stage in toxicity testing as this therapeutic modality is translated to other species.

## Comparative Toxicity: Identification of Target Organs

Since the engineered PrAgs are activated by proteases with differing tissue expression levels, we anticipated that differences might also exist in their off-target toxicities. Bearing this in mind, we performed complete necropsies, with gross and histopathological studies, on toxin-treated mice. We found that independent of the activating protease, the GI tract was the first organ system affected by I.P administered toxins and that in all cases the GI pathology was dose-dependent (Fig. 1).

The first identifiable abnormality, a grossly visible, mild dilation of the small intestine, occurred at doses of 18.75 μg PrAg-L1 + 6.25 μg LF, 37.5 μg PrAg-U2 + 12.5 μg LF and 45 μg IC-PrAg + 15 μg LF, affecting 3/4, 4/9 and 1/10 mice respectively. Further histopathological examination of affected GI tracts confirmed the small intestinal dilation, and identified occasional pockets of focal inflammation with no alterations in villus structure. Mice with this level of GI abnormality exhibited normal behavior during the trial, maintained body weight throughout treatment, and had no identifiable pathology in other tissues examined.

As the doses of each toxin were increased, focal regions of villi with necrotic tips could be identified and inflammation was more diffuse. At the highest doses, pronounced GI changes were apparent, including regions of denuded and/or ulcerated epithelium and gross hemorrhage, which was segmental in nature and selectively affected the small intestine and cecum.

There was no evidence of direct toxicity to other organ systems; however, at doses above those that caused mild GI toxicity, the I.P. toxin injections were consistently associated with dose-dependent peritonitis. In the most severe cases fibrinous peritonitis was observed, and it was not uncommon to identify comorbid conditions such as: necrotizing pancreatitis, liver congestion, venous thrombosis, hypocellular bone marrow and/or thymic depletion. As no evidence of pancreas, liver, heart, bone or thymus pathology was present at lower doses, we speculate that these high dose pathologies occur secondarily to the observed GI lesions and associated inflammation, stress and/or functional deficits.

To determine if the toxin-related GI pathology was an inadvertent consequence of the I.P. route of administration, we also performed necropsies on mice receiving I.V injections. We found that small intestinal dilation was also the earliest toxicity observed when the toxins were administered I.V. and that at the I.V. MTD6s no abnormalities were identified in other organ systems.

### Comparative Toxicity: Mechanism of GI Toxicity

For all three toxin variants, evidence of both direct epithelial damage (villous necrosis) and reduced GI motility (stomach full of ingesta/empty colon) were observed at the highest doses administered. In order to further evaluate the functional significance of these toxicities, we performed charcoal transit assays to assess GI motility in mice treated with either three I.P. or I.V. doses of the least well-tolerated variant, MMP-activated PrAg-L1 + LF (Fig. 2). Importantly, we elected to treat the mice with 3 doses rather than with 6 doses, as used for toxicity determination, in order to ensure that all mice receiving high dose treatments survived the study.

As expected, mice treated with PrAg-L1 + LF at concentrations double its MTD6 (2XMTD6), where GI histopathology was expected, had significantly reduced GI motility. Surprisingly, however, mice treated with the MMP-activated toxin at its I.V. MTD6, a dose below the threshold for GI toxicity, also exhibited a significant reduction in GI motility. This striking finding demonstrates that functional deficiencies can be identified prior to the identification of histopathological alterations, and suggests that PrAg-L1 + LF, and by association the other engineered variants, may be directly toxic to gastrointestinal smooth muscle cells.

### Comparative Efficacy: B16-BL6 Syngraft Model

We next compared the anti-tumor efficacies of the engineered toxin variants using the B16-BL6 model of murine melanoma as it allowed us to perform efficacy testing in the same strain of mice utilized for toxicity characterization. B16-BL6 melanoma is an aggressive and well-characterized cancer that is considered to be a reasonable model of human melanoma as it exhibits overlapping features with the human disease including expression of common melanoma differentiation associated genes, similar immunologic properties, and rapid dissemination to distant organs (Overwijk and Restifo, 2001).

Mice bearing established B16-BL6 syngrafts were treated with six doses of PBS or toxin over the course of two weeks, following the same treatment regimen employed in the toxicity trials. The B16-BL6 tumors grew rapidly, and over the course of the treatment period 55% of mice receiving control, PBS, injections died as a consequence of advanced disease (Fig. 3D–G). We found that PrAg-L1 + LF, PrAg-U2 + LF and IC-PrAg + LF were equally efficient at reducing primary tumor burden when administered at protein equivalent doses (Fig. 3A–C). The greatest anti-tumor effect was achieved using the dual MMP/uPA activated toxin, IC-PrAg + LF, which had a maximal anti-tumor effect of 87% following four doses, and 79% at the conclusion of the trial when administered at its I.P. MTD6 (45 μg IC-PrAg + 15 μg LF) (Fig. 3G). Furthermore, treatment with each of the three toxin variants was observed to improve survival in a dose-dependent manner (Fig. 3D–G).

### Comparative Efficacy: CBC and Blood Chemistry

Terminal blood work was performed on all B16-BL6 melanoma bearing-mice, in order to assess which blood parameters were elevated due to progression of the disease versus which might be elevated as a direct consequence of toxin administration. To determine baseline values, blood was collected from tumor-free mice, which had received sham treatments directly mimicking those of the B16-BL6 bearing cohorts.

As expected, presence of B16-BL6 melanoma caused significant changes in blood work relative to the tumor-free baseline mice (Fig. 4A). Mice bearing B16-BL6 melanoma syngrafts had a mild, non-significant, increase in white blood cell count, which could be accounted for by significant increases in both neutrophil and monocyte populations. Red blood cell values were impacted greatly in the B16-BL6-diseased state, with significant reductions in total red blood cell count, hemoglobin and hematocrit and a significant increase in mean corpuscular volume. A limited blood enzyme panel was also performed, and it was determined that tumor-bearing mice exhibited significant alterations in alkaline phosphatase, alanine aminotransferase, aspartate aminotransferase, creatinine kinase and lactate dehydrogenase levels.

Surprisingly, treatment with any version of the engineered anthrax lethal toxin trended towards normalizing the B16-BL6-dependent blood work changes in a dose-dependent manner (Fig. 4B–C and Supplementary Figs. S1–S2). These data demonstrate that treatment with PrAg-L1 + LF, PrAg-U2 + LF or IC-PrAg + LF not only reduces primary B16-BL6 tumor burden, but also appears to delay progression of tumor-associated morbidities.

Importantly, one toxin-mediated blood work alteration was identified; absolute platelet count was observed to increase in a dose-dependent manner when the engineered toxins were administered (Fig. 4D and Supplementary Fig. S3).

### Comparative Mechanism

We next assessed if there were any mechanistic differences in the anti-tumor mode of action for the MMP-, uPA- or dual MMP/uPA-activated anthrax lethal toxins. B16-BL6 tumors treated with 15 μg PrAg-XX + 5 μg LF were evaluated for necrosis, apoptosis, vessel density and proliferation (Fig. 5). It was observed that all three toxins exerted their anti-tumor effect predominantly through increasing apoptosis, which was found to be 55-, 12-, and 22-fold elevated following treatment with PrAg-L1 + LF, PrAg-U2 + LF and IC-PrAg + LF, respectively (Fig. 5B). Despite differences in the magnitude of apoptotic elevation, the reduction in primary tumor volume for all treatments was indistinguishable (Fig. 5A). This may imply that direct targeting of a specific population of cells is predominantly responsible for the observed anti-tumor effect. Our data suggests that MMPs may be more broadly expressed within the B16-BL6 tumor microenvironment than uPA and that MMP-activity may be present on cell types that are not directly contributing to tumor growth. Accordingly, treatment with either MMP-activated PrAg-L1 + LF or dual MMP/uPA-activated IC-PrAg + LF treatment, results in a greater proportion of cells undergo apoptosis than observed with uPA-activated PrAg-U2 + LF treatment, while the net anti-tumor efficacy remains unchanged.

### Calculation of Therapeutic Index

An estimate of therapeutic index was determined using the following equation: MTD6/ED50, where ED50 was defined as the lowest dose administered where B16-BL6 tumor burden was reduced by a minimum of 50% on study day 14. IC-PrAg + LF was found to have the highest therapeutic index, 9, PrAg-U2 + LF had a therapeutic index of 6, and PrAg-L1 + LF had no separation between its maximum tolerated dose and ED50 with a therapeutic index of 1.

## Discussion

We have previously established that engineered variants of anthrax PrAg can be utilized for the targeted intracellular delivery of cytotoxins. This unique system relies upon proteolytic activation by tumor over-expressed proteases, MMPs and uPA, and we and others have demonstrated that administration of these protease-activated PrAg derivatives, in conjunction with various cytotoxins, can be used to elicit significant *in vivo* anti-tumor responses in diverse cancer models including melanomas, carcinomas and sarcomas (Alfano et al., 2010; Liu et al., 2003b; Liu et al., 2008; Rono et al., 2006; Schafer et al., 2011; Su et al., 2007).

Here we have performed the first in-depth toxicity characterization of MMP-, uPA- and dual MMP/uPA-activated PrAgs, when co-administered with wild-type anthrax lethal factor, LF. We found that independent of the proteolytic-activation site the GI tract is the primary target for toxicity. This toxicity is dose-dependent and is seen following both I.P. and I.V. administration of the engineered toxins. This is consistent with the mechanism of action of these agents, as while both MMPs and uPA are tightly regulated in normal homeostatic tissues, they are both expressed during tissue remodeling and repair (Johnsen et al., 1998). Therefore the presence of active MMPs and uPA in the GI tract, resulting in some off-target activation, is not unexpected.

Following appearance of initial GI pathology, we have further identified that mice treated intraperitoneally with the engineered toxins consistently developed dose-dependent peritonitis. At this time, it remains unclear if this is a sequela to the GI toxicity, an unidentified direct toxicity, or a consequence of the I.P. route of administration. We now know that small intestinal dilation is the first observed pathology in mice treated with the engineered toxins. This GI dilation may increase the risk of needle perforation of the intestines during I.P. administration; intestinal perforation being a well-known risk factor for peritonitis. In this study, we did not see any evidence of chronic peritonitis in mice treated with the engineered toxins I.V., but necropsies were not performed at high doses exceeding the I.V. MTD6s where this manifestation of toxicity might be expected.

Additionally, we have presented preliminary evidence that I.P. or I.V. administration of an MMP-activated anthrax lethal toxin, PrAg-L1 + LF, is associated with reduction in GI motility at doses below those where histopathological abnormalities are first observed. This finding suggests that GI smooth muscle cells may be directly targeted by the engineered toxins, and ongoing investigations in our laboratory focus on further exploring this toxicity. Characterization of the cellular targets of the observed GI toxicity is relevant not only to the

continued development of our experimental agents, but may also be applicable to the pathogenesis of wild-type anthrax lethal toxin. While the primary toxicity associated with wild-type toxin is hemodynamic shock and cardiovascular collapse (Cui et al., 2004; Golden et al., 2009; Liu et al., 2013) reports of gastrointestinal toxicity have occasionally been made in mice treated systemically with purified wild-type toxin (Abi-Habib et al., 2006; Fang et al., 2010; Moayeri et al., 2003; Okugawa et al., 2011; Sun et al., 2012). In 2012, Sun et al. found that I.V. administration of sub-lethal doses of wild-type anthrax lethal toxin (~LD50) led to delayed onset GI toxicity within the surviving population that was strikingly similar in appearance to that reported herein, characterized by edema of the small intestine, villous necrosis, mucosal erosion and ulceration, and gross hemorrhage (Sun et al., 2012). While Sun et al., provide compelling evidence that their observed GI toxicity is a manifestation of direct epithelial damage, evidence also exists suggesting that this GI toxicity might instead be a consequence of GI smooth muscle injury, as Abi-Habib et al. reported that systemic administration of wild-type anthrax lethal toxin resulted in the development of fatal paralytic ileus without any alterations in intestinal histology (Abi-Habib et al., 2006). In our current study, mice treated with the highest doses of engineered toxin had evidence of both reduced GI motility (full stomach/empty colon on gross necropsy) and epithelial damage (villous necrosis, denuded/ulcerated GI epithelia); however, at doses below those where histopathological changes were first observed functional reductions in GI motility were seen in mice treated with our most toxic engineered variant, MMP-activated PrAg-L1 + LF. Continued research is in progress to further evaluate the cellular target of our engineered toxin variants, with specific focus on our most promising candidate, dual MMP/uPA-activated IC-PrAg + LF, and application to wild-type PrAg-WT + LF.

During the course of our efficacy studies, we became aware of one additional toxin-dependent change: Tumor-bearing mice treated I.P. with the MMP-, uPA- or dual MMP/uPA-activated toxins displayed a dose-dependent increase in absolute platelet count. The clinical relevance of this mild reactive thrombocytosis is unclear; however, this effect should certainly be kept in mind as further characterization is performed on these agents. Platelet count should likely be monitored with treatment, and it is possible that recipients would benefit from prophylactic administration of an anti-coagulant, such as aspirin, to reduce risk of thrombosis, the primary complication associated with thrombocytotic state.

With regard to efficacy, we found that each of the three toxin variants lead to significant reduction in primary B16-BL6 tumor burden and delayed progression of disease-related morbidities in a dose-dependent manner. Each toxin exhibited similar activity when administered at protein equivalent doses and in all cases the primary mechanism of tumoricidal activity was increased apoptosis. While target-organ toxicity and efficacy were similar amongst the variants, IC-PrAg + LF, an engineered anthrax lethal toxin requiring co-localized activation by both MMPs and uPA, emerged as the best candidate exhibiting the highest MTD6 and the highest threshold for target-organ toxicity, while maintaining significant anti-tumor efficacy.

While we demonstrate here that IC-PrAg + LF has significant anti-tumor activity towards B16-BL6 melanoma, it is relevant to note that a highly similar toxin combination, IC-PrAg + LF-HMAGG (a version of wild-type anthrax LF containing two non-native amino acids,

HM, at its N-terminus), has been previously documented to exhibit potent *in vivo* activity towards HN12, HN6, Hep2 and Cal27 head and neck squamous cell carcinoma xenografts (Schafer et al., 2011). Given the strong similarities between these two toxin combinations, it is highly likely that IC-PrAg + LF will also exhibit broad anti-tumor efficacy, and this expectation, paired with our current demonstration that effective doses can be administered far below the threshold for toxicity, supports the assertion that IC-PrAg + LF is a highly promising candidate for further development as an anti-cancer agent.

## Supplementary Material

Refer to Web version on PubMed Central for supplementary material.

## Acknowledgments

The authors thank Rasem Fattah for toxin purification. Financial support for this study was provided by the NIDCR Intramural Research Program (T.H.B) and the NIAID Intramural Research Program (S.H.L.)

## References

1. Andreasen PA, Kjoller L, Christensen L, Duffy MJ. The urokinase-type plasminogen activator system in cancer metastasis: a review. Int J Cancer. 1997; 72:1–22. [PubMed: 9212216]
2. Bugge, TH. Proteolysis in carcinogenesis. In: Ensley, JF.; Gutkind, JS.; Jacob, JR.; Lippman, SM., editors. Head and Neck Cancer. Academic Press; San Diego: 2003. p. 137-49.
3. Duffy MJ, Mullooly M, O'Donovan N, Sukor S, Crown J, Pierce A, McGowan PM. The ADAMs family of proteases: new biomarkers and therapeutic targets for cancer? Clin Proteomics. 2011; 8:9. [PubMed: 21906355]
4. Kontos CK, Scorilas A. Kallikrein-related peptidases (KLKs): a gene family of novel cancer biomarkers. Clin Chem Lab Med. 2012; 50:1877–91. [PubMed: 23093268]
5. Roy R, Yang J, Moses MA. Matrix metalloproteinases as novel biomarkers and potential therapeutic targets in human cancer. J Clin Oncol. 2009; 27:5287–97. [PubMed: 19738110]
6. Liu S, Netzel-Arnett S, Birkedal-Hansen H, Leppla SH. Tumor cell-selective cytotoxicity of matrix metalloproteinase-activated anthrax toxin. Cancer Res. 2000; 60:6061–7. [PubMed: 11085528]
7. Liu S, Bugge TH, Leppla SH. Targeting of tumor cells by cell surface urokinase plasminogen activator-dependent anthrax toxin. J Biol Chem. 2001; 276:17976–84. [PubMed: 11278833]
8. Liu S, Redeye V, Kuremsky JG, Kuhnen M, Molinolo A, Bugge TH, Leppla SH. Intermolecular complementation achieves high-specificity tumor targeting by anthrax toxin. Nat Biotechnol. 2005; 23:725–30. [PubMed: 15895075]
9. Liu S, Schubert RL, Bugge TH, Leppla SH. Anthrax toxin: structures, functions and tumour targeting. Expert Opin Biol Ther. 2003a; 3:843–53. [PubMed: 12880383]
10. Bradley KA, Mogridge J, Mourez M, Collier RJ, Young JA. Identification of the cellular receptor for anthrax toxin. Nature. 2001; 414:225–9. [PubMed: 11700562]
11. Liu S, Crown D, Miller-Randolph S, Moayeri M, Wang H, Hu H, Morley T, Leppla SH. Capillary morphogenesis protein-2 is the major receptor mediating lethality of anthrax toxin in vivo. Proc Natl Acad Sci U S A. 2009; 106:12424–9. [PubMed: 19617532]
12. Scobie HM, Rainey GJ, Bradley KA, Young JA. Human capillary morphogenesis protein 2 functions as an anthrax toxin receptor. Proc Natl Acad Sci U S A. 2003; 100:5170–4. [PubMed: 12700348]
13. Klimpel KR, Molloy SS, Thomas G, Leppla SH. Anthrax toxin protective antigen is activated by a cell surface protease with the sequence specificity and catalytic properties of furin. Proc Natl Acad Sci U S A. 1992; 89:10277–81. [PubMed: 1438214]

14. Cunningham K, Lacy DB, Mogridge J, Collier RJ. Mapping the lethal factor and edema factor binding sites on oligomeric anthrax protective antigen. Proc Natl Acad Sci U S A. 2002; 99:7049–53. [PubMed: 11997439]
15. Mogridge J, Cunningham K, Lacy DB, Mourez M, Collier RJ. The lethal and edema factors of anthrax toxin bind only to oligomeric forms of the protective antigen. Proc Natl Acad Sci U S A. 2002; 99:7045–8. [PubMed: 11997437]
16. Duesbery NS, Webb CP, Leppla SH, Gordon VM, Klimpel KR, Copeland TD, Ahn NG, Oskarsson MK, Fukasawa K, Paull KD, Vande Woude GF. Proteolytic inactivation of MAP-kinase-kinase by anthrax lethal factor. Science. 1998; 280:734–7. [PubMed: 9563949]
17. Vitale G, Pellizzari R, Recchi C, Napolitani G, Mock M, Montecucco C. Anthrax lethal factor cleaves the N-terminus of MAPKKs and induces tyrosine/threonine phosphorylation of MAPKs in cultured macrophages. Biochem Biophys Res Commun. 1998; 248:706–11. [PubMed: 9703991]
18. Vitale G, Bernardi L, Napolitani G, Mock M, Montecucco C. Susceptibility of mitogen-activated protein kinase kinase family members to proteolysis by anthrax lethal factor. Biochem J. 2000; 352(Pt 3):739–45. [PubMed: 11104681]
19. Alfano RW, Leppla SH, Liu S, Bugge TH, Ortiz JM, Lairmore TC, Duesbery NS, Mitchell IC, Nwariaku F, Frankel AE. Inhibition of tumor angiogenesis by the matrix metalloproteinase-activated anthrax lethal toxin in an orthotopic model of anaplastic thyroid carcinoma. Mol Cancer Ther. 2010; 9:190–201. [PubMed: 20053778]
20. Liu S, Aaronson H, Mitola DJ, Leppla SH, Bugge TH. Potent antitumor activity of a urokinase-activated engineered anthrax toxin. Proc Natl Acad Sci U S A. 2003b; 100:657–62. [PubMed: 12525700]
21. Liu S, Wang H, Currie BM, Molinolo A, Leung HJ, Moayeri M, Basile JR, Alfano RW, Gutkind JS, Frankel AE, Bugge TH, et al. Matrix metalloproteinase-activated anthrax lethal toxin demonstrates high potency in targeting tumor vasculature. J Biol Chem. 2008; 283:529–40. [PubMed: 17974567]
22. Rono B, Romer J, Liu S, Bugge TH, Leppla SH, Kristjansen PE. Antitumor efficacy of a urokinase activation-dependent anthrax toxin. Mol Cancer Ther. 2006; 5:89–96. [PubMed: 16432166]
23. Schafer JM, Peters DE, Morley T, Liu S, Molinolo AA, Leppla SH, Bugge TH. Efficient targeting of head and neck squamous cell carcinoma by systemic administration of a dual uPA and MMP-activated engineered anthrax toxin. PLoS One. 2011; 6:e20532. [PubMed: 21655226]
24. Su Y, Ortiz J, Liu S, Bugge TH, Singh R, Leppla SH, Frankel AE. Systematic urokinase-activated anthrax toxin therapy produces regressions of subcutaneous human non-small cell lung tumor in athymic nude mice. Cancer Res. 2007; 67:3329–36. [PubMed: 17409442]
25. Wein AN, Liu S, Zhang Y, McKenzie AT, Leppla SH. Tumor therapy with a urokinase plasminogen activator-activated anthrax lethal toxin alone and in combination with paclitaxel. Invest New Drugs. 2013; 31:206–12. [PubMed: 22843210]
26. Alfano RW, Leppla SH, Liu S, Bugge TH, Duesbery NS, Frankel AE. Potent inhibition of tumor angiogenesis by the matrix metalloproteinase-activated anthrax lethal toxin: implications for broad anti-tumor efficacy. Cell Cycle. 2008; 7:745–9. [PubMed: 18245947]
27. Klimpel KR, Arora N, Leppla SH. Anthrax toxin lethal factor contains a zinc metalloprotease consensus sequence which is required for lethal toxin activity. Mol Microbiol. 1994; 13:1093–100. [PubMed: 7854123]
28. Park S, Leppla SH. Optimized production and purification of Bacillus anthracis lethal factor. Protein Expr Purif. 2000; 18:293–302. [PubMed: 10733882]
29. Tomayko MM, Reynolds CP. Determination of subcutaneous tumor size in athymic (nude) mice. Cancer Chemother Pharmacol. 1989; 24:148–54. [PubMed: 2544306]
30. Overwijk WW, Restifo NP. B16 as a mouse model for human melanoma. Curr Protoc Immunol. 2001; Chapter 20(Unit 20.1)
31. Johnsen M, Lund LR, Romer J, Almholt K, Dano K. Cancer invasion and tissue remodeling: common themes in proteolytic matrix degradation. Curr Opin Cell Biol. 1998; 10:667–71. [PubMed: 9818179]
32. Cui X, Moayeri M, Li Y, Li X, Haley M, Fitz Y, Correa-Araujo R, Banks SM, Leppla SH, Eichacker PQ. Lethality during continuous anthrax lethal toxin infusion is associated with

circulatory shock but not inflammatory cytokine or nitric oxide release in rats. Am J Physiol Regul Integr Comp Physiol. 2004; 286:R699–709. [PubMed: 14715494]

33. Golden HB, Watson LE, Lal H, Verma SK, Foster DM, Kuo SR, Sharma A, Frankel A, Dostal DE. Anthrax toxin: pathologic effects on the cardiovascular system. Front Biosci. 2009; 14:2335–57.
34. Liu S, Zhang Y, Moayeri M, Liu J, Crown D, Fattah RJ, Wein AN, Yu ZX, Finkel T, Leppla SH. Key tissue targets responsible for anthrax-toxin-induced lethality. Nature. 2013; 501:63–8. [PubMed: 23995686]
35. Abi-Habib RJ, Singh R, Leppla SH, Greene JJ, Ding Y, Berghuis B, Duesbery NS, Frankel AE. Systemic anthrax lethal toxin therapy produces regressions of subcutaneous human melanoma tumors in athymic nude mice. Clin Cancer Res. 2006; 12:7437–43. [PubMed: 17189417]
36. Fang H, Sun C, Xu L, Owen RJ, Auth RD, Snoy PJ, Frucht DM. Neutrophil elastase mediates pathogenic effects of anthrax lethal toxin in the murine intestinal tract. J Immunol. 2010; 185:5463–7. [PubMed: 20921524]
37. Moayeri M, Haines D, Young HA, Leppla SH. Bacillus anthracis lethal toxin induces TNF-alpha-independent hypoxia-mediated toxicity in mice. J Clin Invest. 2003; 112:670–82. [PubMed: 12952916]
38. Okugawa S, Moayeri M, Eckhaus MA, Crown D, Miller-Randolph S, Liu S, Akira S, Leppla SH. MyD88-dependent signaling protects against anthrax lethal toxin-induced impairment of intestinal barrier function. Infect Immun. 2011; 79:118–24. [PubMed: 20974827]
39. Sun C, Fang H, Xie T, Auth RD, Patel N, Murray PR, Snoy PJ, Frucht DM. Anthrax lethal toxin disrupts intestinal barrier function and causes systemic infections with enteric bacteria. PLoS One. 2012; 7:e33583. [PubMed: 22438953]

## Highlights

- Toxicity and anti-tumor activity of protease-activated anthrax toxins were evaluated.
- All anthrax toxin variants exhibited potent systemic anti-tumor activity in mice.
- A dual MMP/uPA-activated anthrax toxin displayed a superior safety profile.
- Clinical development of a dual MMP/uPA-activated anthrax toxin is feasible.

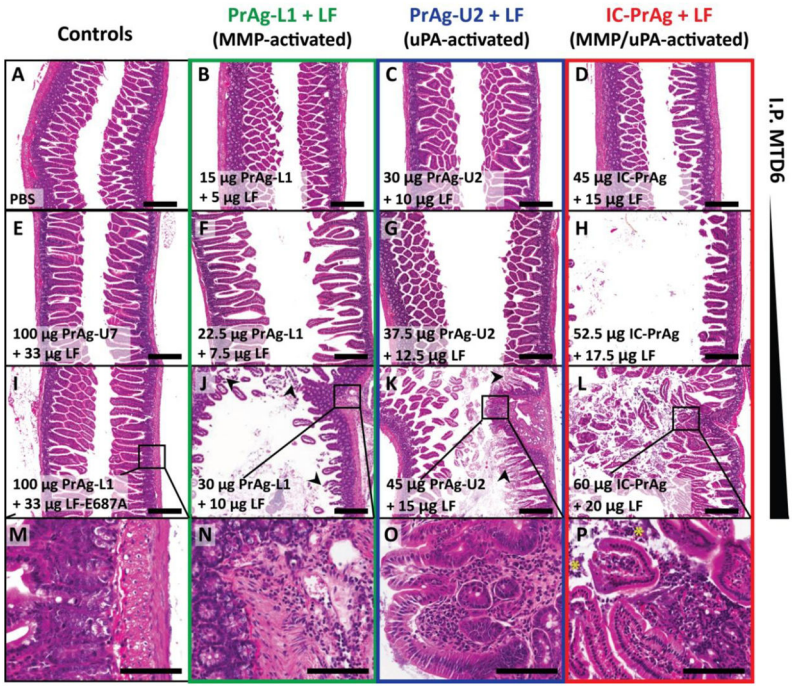


**Figure 1. GI toxicity is dose-limiting when C57BL/6J mice are treated with six I.P. doses of MMP-, uPA- or dual MMP/uPA-activated anthrax lethal toxins**

Representative H&E sections of small intestine depicting the dose-dependent progression of GI toxicity observed when PrAg-L1 + LF (B,F,J,N) PrAg-U2 + LF (C,G,K,O) or IC-PrAg + LF (D,H,L,P) are administered intraperitoneally. At the MTD6 for each toxin, no GI pathology was present at the gross or microscopic level in 29/30 experimental mice (B–D). At this dose, note the similarity in appearance to control-treated mice receiving 6 I.P. doses of either PBS (A), uncleavable anthrax PrAg paired with LF, 100 µg PrAg-U7 + 33 µg LF (E), or MMP-activated PrAg paired with enzymatically-inactive cytotoxin, 100 µg PrAg-L1 + 33 µg LF-E687A (I). As doses were increased above the MTD6, GI toxicity initially presented as mild small intestinal dilation (F–H) which progressed in severity to involve GI inflammation, regions of villous necrosis, denuded and ulcerated GI epithelium and/or grossly visible GI hemorrhage (J–L, arrowheads depict necrotic villi). (M–P) Higher magnification images showing inflammation in the lamina propria of toxin-treated mice, but not controls. (P) * indicates inflammatory cells that have invaded into the lumen of the small intestine. Scale bars are 300 µm A–L; 100 µm M–P.

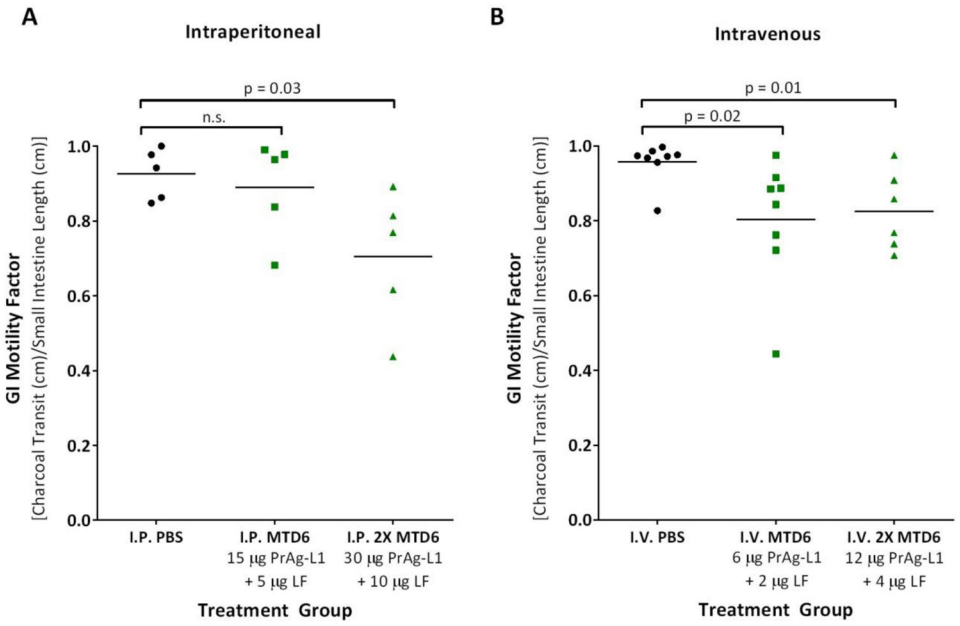


**Figure 2. I.P. or I.V. treatment with MMP-activated PrAg-L1 + LF caused reduced GI motility**

3 doses of PBS (black) or PrAg-L1 + LF (green) were administered either intraperitoneally (A) or intravenously (B). At both the I.P. and I.V. MTD6s, no physical evidence of GI abnormalities was anticipated, while at doses of 2XMTD6 GI histopathology was expected. P-values were determined using a Student's T-test, two-tailed.

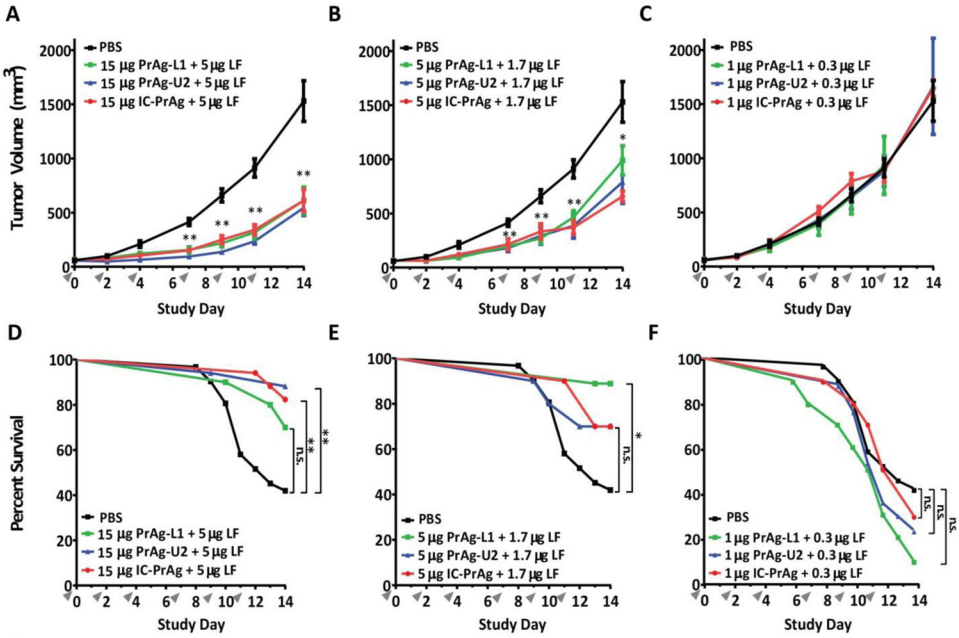


G

| Description of Agent | | Dose (µg) | Dose / MTD6 | n | Maximum % Tumor Reduction | | % Tumor Reduction at Day 14 | | % Survival at Day 14 | |
|---|---|---|---|---|---|---|---|---|---|---|
| vehicle control | PBS | --- | --- | 31 | --- | --- | --- | --- | 45 | --- |
| MMP-activated anthrax toxin | PrAg-L1 + LF | 15/5 | 1 | 10 | 66 | [d.11] | 62 | ** | 70 | n.s. |
| | | 5/1.7 | 1/3 | 10 | 56 | [d.9] | 32 | * | 90 | * |
| | | 1/0.3 | 1/15 | 10 | 0 | --- | 0 | n.s. | 10 | n.s. |
| uPA-activated anthrax toxin | PrAg-U2 + LF | 24.3/8.1 | 4/5 | 10 | 75 | [d.9] | 63 | ** | 100 | ** |
| | | 15/5 | 1/2 | 17 | 78 | [d.9] | 66 | ** | 94 | ** |
| | | 5/1.7 | 1/6 | 10 | 59 | [d.11] | 50 | * | 70 | n.s. |
| | | 1/0.3 | 1/30 | 17 | 0 | --- | 0 | n.s. | 24 | n.s. |
| dual MMP/uPA-activated anthrax toxin | IC-PrAg [PrAg-L1-I210A + PrAg-U2-R200A] + LF | 22.5/22.5/15 | 1 | 10 | 87 | [d.9] | 79 | ** | 70 | n.s. |
| | | 7.5/7.5/5 | 1/3 | 17 | 64 | [d.11] | 62 | ** | 82 | ** |
| | | 2.5/2.5/1.7 | 1/9 | 10 | 60 | [d.11] | 59 | * | 70 | n.s. |
| | | 0.5/0.5/0.3 | 1/45 | 10 | 0 | --- | 0 | n.s. | 30 | n.s. |

**Figure 3. Engineered anthrax lethal toxins reduce B16-BL6 tumor burden and improve survival in a dose-dependent manner**

(A–C) Tumor growth and (D–F) survival of C57BL/6J mice bearing B16-BL6 melanoma syngrafts that were treated with six I.P. doses of either PBS (black lines) or engineered anthrax lethal toxins, MMP-activated PrAg-L1 + LF (green), uPA-activated PrAg-U2 + LF (blue) or dual MMP/uPA-activated IC-PrAg + LF (red), at time points indicated by grey arrowheads. All cohorts were treated in parallel and the PBS control groups depicted in panels A–C and D–F are the same. Note that the anti-tumor effect was independent of the proteolytic-activation site; PrAg-L1 + LF, PrAg-U2 + LF and IC-PrAg + LF exhibited indistinguishable anti-tumor effects when administered at protein equivalent doses (A–C). Tumor volume data are expressed as mean tumor weight ± standard error of the mean; *, $P<0.05$, **, $P<0.01$, Student's two-tailed t-test. (D–F) Kaplan-Meier survival curves were compared via Log-Rank test; *, $P<0.05$, **, $P<0.01$. (G) Table summarizing anti-tumor and survival effects associated with engineered toxin administration. Abbreviations: n = mouse number, [d.X] = trial day on which maximum % tumor reduction was observed. P-value for % tumor reduction on day 14 was calculated in comparison to the control PBS-treated tumor

cohort using a two-tailed Student's t-test; *, P<0.05, **, P<0.01. P-value for % survival was calculated by comparing Kaplan-Meier survival curves of experimental cohorts with that of the PBS-treated cohort using the Log-Rank test, two-tailed;*, P<0.05, **, P<0.01.

A

| Bloodwork Parameter | | | Treatment Group: Tumor-Free PBS (n=9) Median | Treatment Group: B16-BL6 Tumor PBS (n=7) Median | P |
|---|---|---|---|---|---|
| Complete Blood Count | Absolute White Blood Cell Count [WBC] | K/μL | 6.2 | 11.4 | n.s. |
| | Absolute Neutrophil Count | K/μL | 0.4 | 1.7 | ** |
| | Absolute Lymphocyte Count | K/μL | 5.6 | 7.8 | n.s. |
| | Absolute Monocyte Count | K/μL | 0.16 | 0.37 | * |
| | Absolute Eosinophil Count | K/μL | 0.08 | 0.05 | n.s. |
| | Absolute Basophil Count | K/μL | 0.33 | 0.27 | n.s. |
| | Absolute Red Blood Cell Count [RBC] | M/μL | 9.6 | 3.75 | ** |
| | Hemoglobin [Hmg] | g/dL | 14.6 | 7.2 | ** |
| | Hematocrit [Hct] | % | 43.3 | 20.7 | ** |
| | Mean Corpuscular Volume [MCV] | K/μL | 45.1 | 47.5 | * |
| | Absolute Platelet Count | K/μL | 835 | 792 | n.s. |
| Chemistry | Alkaline Phosphatase [ALP] | U/L | 175 | 52 | *** |
| | Alanine Aminotransferase [ALT] | U/L | 43 | 142 | *** |
| | Aspartate Aminotransferase [AST] | U/L | 103 | 735 | *** |
| | Amylase [AMY] | U/L | 2872 | 2712 | n.s. |
| | Creatine Kinase [CK] | U/L | 167 | 643 | * |
| | Lactate Dehydrogenase [LD] | U/L | 329 | 2218 | *** |

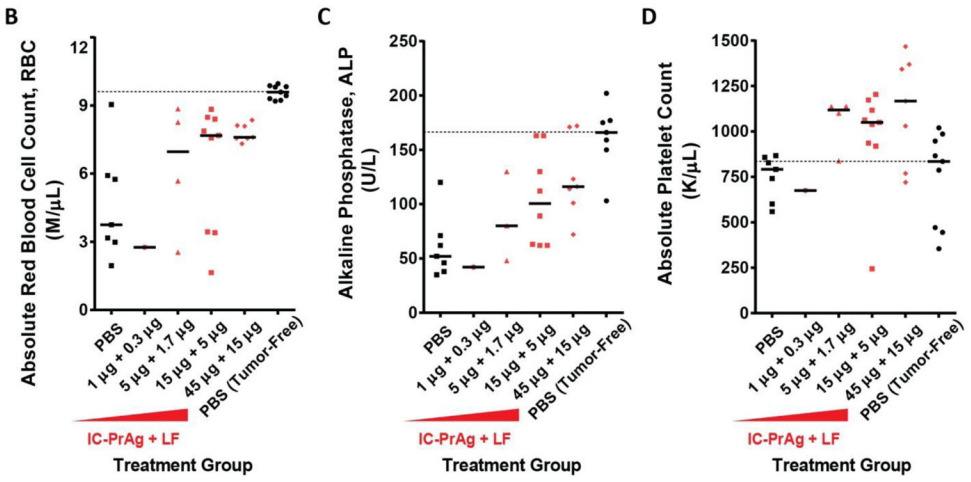


**Figure 4. Treatment of B16-BL6 melanoma-bearing mice with a dual MMP/uPA-activated anthrax lethal toxin leads to normalization of blood work values**

B16-BL6 melanoma caused significant changes in complete blood count and blood chemistry values relative to tumor-free mice receiving otherwise identical treatments (A). Administration of IC-PrAg + LF led to dose dependent normalization of absolute red blood cell count (B) and alkaline phosphatase levels (C). One toxin-dependent change in blood work values was observed; Treatment with IC-PrAg + LF led to a dose-dependent elevation in absolute platelet count (D). (A) Student's t-test, two-tailed;*, P<0.05;**, P<0.01;***, P<0.001. (B–D) Bars indicate medians, dashed line indicates disease-free median.

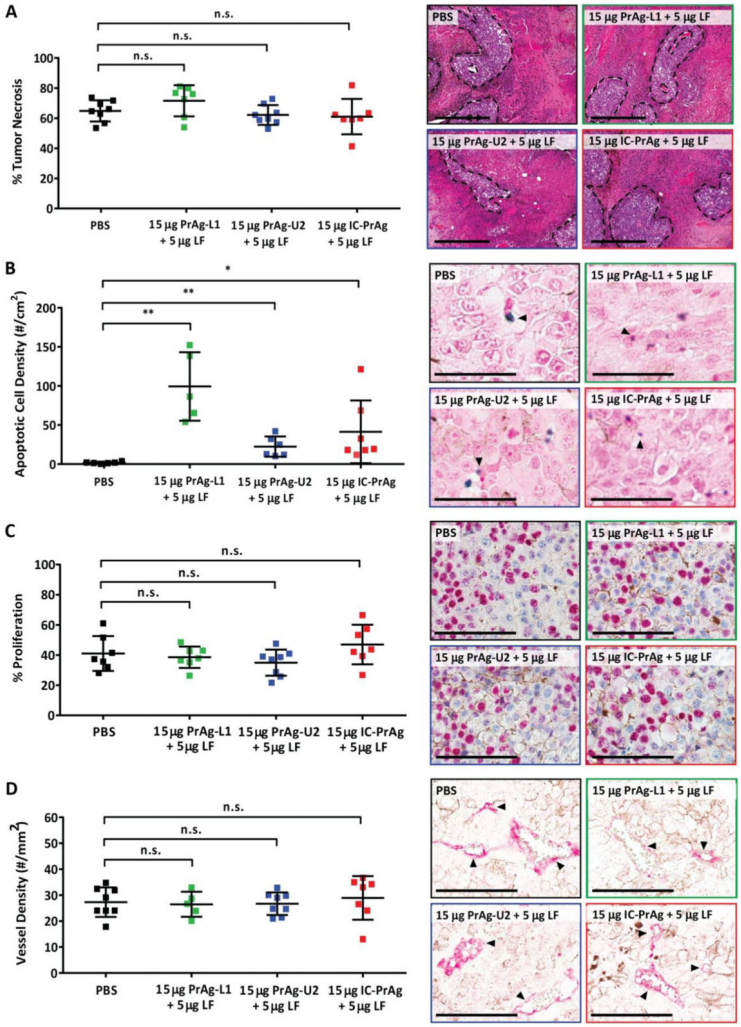


**Figure 5. Mechanism of tumoricidal activity of engineered anthrax toxins**

Quantification of necrosis (A), apoptosis (B), proliferation (C) and vessel density (D) in B16-BL6 tumors harvested from mice treated with 6 I.P. doses of engineered anthrax lethal toxins at a concentration of 15 µg engineered PrAg + 5 µg LF. In all panels: PBS (black), MMP-activated PrAg-L1 + LF (green), uPA-activated PrAg-U2 + LF (blue) and dual MMP/uPA-activated IC-PrAg + LF (red). (A–D) Student's two-tailed t-test; **, P<0.01. (A, right) H&E stain. Regions of viable cells are outlined with black dashed lines, scale bars = 500 µm. (B, right) TUNEL stain. Arrowheads highlight examples of TdT positive apoptotic cells stained with TACS blue label, scale bars = 100 µm. (C, right) Ki67 positive nuclei are stained pink with Vulcan FastRed, scale bars = 100 µm. (D, right) Arrowheads highlight CD31 positive blood vessels stained with Vuclan FastRed, scale bars = 100 µm. In all cases representative images are shown.

## Table 1

Literature summary of *in vivo* tumor models where significant anti-tumor efficacy was reported when engineered PrAgs were administered in combination with various cytotoxins

| Engineered PrAg | Cytotoxin | *In vivo* Tumor Model |
|---|---|---|
| **MMP-activated PrAg, PrAg-L1** | **LF-HMAGG**[b] | LL3, Lewis lung carcinoma syngraft (22) |
| | | B16-BL6, melanoma syngraft (22) |
| | | C32, melanoma xenograft (22) |
| | | HT144, melanoma xenograft (22) |
| | | A549, lung carcinoma xenograft (22) |
| | | Colo205, colon carcinoma xenograft (22) |
| | | BHT-101, anaplastic thyroid carcinoma orthotopic implant (23) |
| **uPA-activated PrAg, PrAg-U2** | **FP59**[c] | LL3, Lewis lung carcinoma syngraft (19,20) |
| | | T241, fibrosarcoma syngraft (19,20) |
| | | B16-BL6, melanoma syngraft (19,20) |
| | | HT1299, non-squamous cell lung carcinoma xenograft (21) |
| | **LF**[a] | B16-BL6, melanoma syngraft (25) |
| **dual MMP/uPA-activated PrAg, IC-PrAg (PrAg-L1-I210A + PrAg-U2-R200A)** | **FP59**[c] | LL3, Lewis lung carcinoma syngraft (8) |
| | | T241, fibrosarcoma syngraft (8) |
| | | B16-BL6, melanoma syngraft (8) |
| | **LF-HMAGG**[b] | HN12, head and neck squamous cell carcinoma xenograft (24) |
| | | HN6, head and neck squamous cell carcinoma (24) |
| | | Hep2, head and neck squamous cell carcinoma (24) |
| | | Cal27, head and neck squamous cell carcinoma (24) |

[a] LF is wild-type anthrax lethal factor, with the native N-terminal sequence AGG

[b] LF-HMAGG is a version of LF having the non-native N-terminal sequence HMAGG

[c] FP59 is a fusion protein containing the PrAg binding domain of LF fused to the catalytic domain of *Pseudomonas aeruginosa* exotoxin A

*Toxicol Appl Pharmacol*. Author manuscript; available in PMC 2015 September 01.

**Table 2**

Mortality associated with I.P. administration of engineered anthrax lethal toxins: Determining I.P. MTD6

| Description of Agent | | | Dose (μg) | # Mice | % Survival at Day 14 | Log-Rank[a] (P) |
|---|---|---|---|---|---|---|
| **Control Groups** | vehicle control | PBS | --- | 10 | 100 | --- |
| | wild-type anthrax lethal toxin | PrAg-WT + LF | 15/5 | 10 | 0 | < 0.01 |
| | uncleavable anthrax lethal toxin | PrAg-U7 + LF | 100/33.3 | 5 | 100 | n.s. |
| | MMP-activated PrAg alone | PrAg-L1 | 100 | 5 | 100 | n.s. |
| | uPA-activated PrAg alone | PrAg-U2 | 100 | 5 | 100 | n.s. |
| | dual MMP/uPA-activated PrAg alone | IC-PrAg (PrAg-L1-I210A + PrAg-U2-R200A) | 100 | 5 | 100 | n.s. |
| | MMP-activated PrAg + enzymatically-inactive LF | PrAg-L1 + LF-E687A | 100/33.3 | 5 | 100 | n.s. |
| | uPA-activated PrAg + enzymatically-inactive LF | PrAg-U2 + LF-E687A | 100/33.3 | 5 | 100 | n.s. |
| | dual MMP/uPA-activated PrAg + enzymatically-inactive LF | IC-PrAg (PrAg-L1-I210A + PrAg-U2-R200A) + LF-E687A | 50/50/33.3 | 5 | 100 | n.s. |
| **Experimental Groups [I.P. MTD6 Determination]** | MMP-activated anthrax lethal toxin | PrAg-L1 + LF | 30/10 | 5 | 60 | 0.03 |
| | | | 22.5/7.5 | 5 | 60 | 0.03 |
| | | | 18.75/6.25 | 5 | 80 | n.s. |
| | | | 15/5[b] | 10 | 100 | n.s. |
| | uPA-activated anthrax lethal toxin | PrAg-U2 + LF | 45/15 | 10 | 80 | n.s. |
| | | | 37.5/12.5 | 10 | 90 | n.s. |
| | | | 30/10[b] | 10 | 100 | n.s. |
| | dual MMP/uPA-activated anthrax lethal toxin | IC-PrAg (PrAg-L1-I210A + PrAg-U2-R200A) + LF | 30/30/20 | 10 | 60 | 0.03 |
| | | | 26.2/26.2/17.5 | 5 | 80 | n.s. |
| | | | 22.5/22.5/15 [b] | 10 | 100 | n.s. |
| | | | 15/15/10 | 5 | 100 | n.s. |

[a] Log-Rank tests compare the Kaplan-Meier survival curve of the vehicle control (PBS) cohort with that of the indicated cohort

[b] I.P. MTD6

Abbreviations: n.s., not significant

**Table 3**

Mortality associated with I.V. administration of engineered anthrax lethal toxins: Determining I.V. MTD6

| | Description of Agent | | Dose (μg) | # Mice | % Survival at Day 14 | Log-Rank[a] (P) |
|---|---|---|---|---|---|---|
| **Control Groups** | vehicle control | PBS | --- | 10 | 100 | --- |
| | wild-type anthrax lethal toxin | PrAg-WT + LF | 6/2 | 5 | 0 | <0.01 |
| | MMP-activated PrAg + enzymatically-inactive LF | PrAg-L1 + LF-E687A | 50/16.7 | 6 | 50 | 0.01 |
| | MMP-activated PrAg alone | PrAg-L1 | 50 | 5 | 60 | 0.03 |
| | uPA-activated PrAg alone | PrAg-U2 | 50 | 4 | 75 | n.s. |
| | dual MMP/uPA-activated PrAg alone | IC-PrAg (PrAg-L1-I210A + PrAg-U2-R200A) | 25/25 | 5 | 80 | n.s. |
| **Experimental Groups [I.V. MTD6 Determination]** | MMP-activated anthrax lethal toxin | PrAg-L1 + LF | 15/5 | 4 | 0 | <0.01 |
| | | | 12/4 | 9 | 66 | 0.02 |
| | | | 9/3 | 10 | 70 | n.s. |
| | | | 6/2[b] | 10 | 100 | n.s. |
| | | | 3/1 | 6 | 100 | n.s. |
| | uPA-activated anthrax lethal toxin | PrAg-U2 + LF | 15/5 | 8 | 75 | n.s. |
| | | | 12/4[b] | 13 | 100 | n.s. |
| | | | 9/3 | 11 | 100 | n.s. |
| | Dual MMP/uPA-activated anthrax lethal toxin | IC-PrAg (PrAg-L1-I210A + PrAg-U2-R200A) + LF | 7.5/7.5/5 | 5 | 80 | n.s. |
| | | | 6/6/4[b] | 12 | 100 | n.s. |
| | | | 4.5/4.5/3 | 11 | 100 | n.s. |

[a] Log-Rank tests compare the Kaplan-Meier survival curve of the vehicle control (PBS) cohort with that of the indicated cohort

[b] I.V. MTD6

Abbreviations: n.s., not significant